

This paper is published as part of a *Dalton Transactions* theme issue:

Dalton Discussion 11: The Renaissance of Main Group Chemistry

Guest Editor: John Arnold
University of California, Berkeley, CA, USA
23 - 25 June 2008

Published in [issue 33, 2008](#), of *Dalton Transactions*

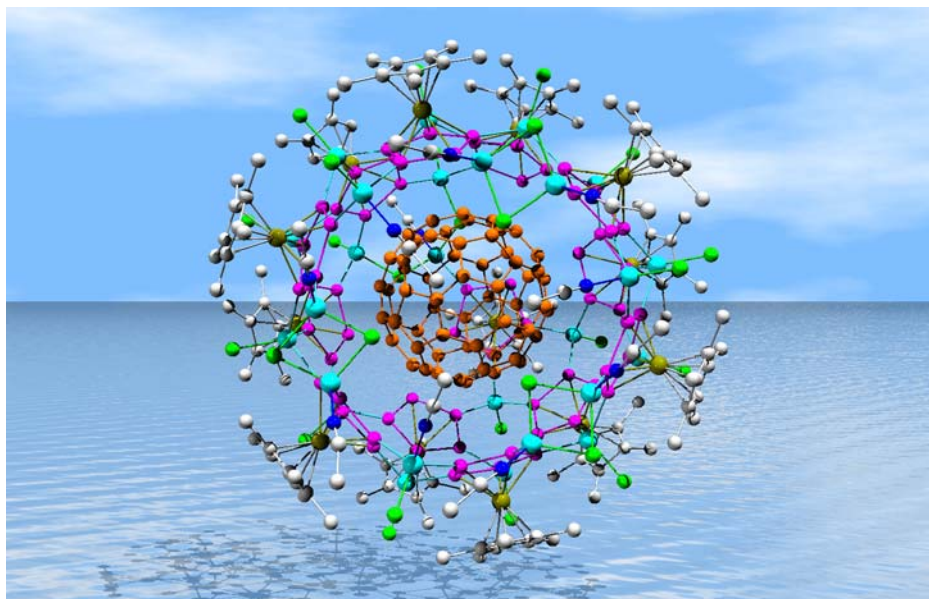


Image reproduced with permission of Manfred Scheer

Papers published in this issue include:

[The coordination chemistry of group 15 element ligand complexes—a developing area](#)

Manfred Scheer, *Dalton Trans.*, 2008 DOI: [10.1039/b718179p](#)

[Formation, structure and bonding of metalloid Al and Ga clusters. A challenge for chemical efforts in nanosciences](#)

Hansgeorg Schnöckel, *Dalton Trans.*, 2008 DOI: [10.1039/b718784j](#)

[Polymeric materials based on main group elements: the recent development of ambient temperature and controlled routes to polyphosphazenes](#)

Vivienne Blackstone, Alejandro Presa Soto and Ian Manners, *Dalton Trans.*, 2008
DOI: [10.1039/b719361k](#)

[Recent developments in the chemistry of low valent Group 14 hydrides](#)

Eric Rivard and Philip P. Power, *Dalton Trans.*, 2008 DOI: [10.1039/b801400k](#)

[Chemistry and physics of silicon nanowire](#)

Peidong Yang, *Dalton Trans.*, 2008 DOI: [10.1039/b801440j](#)

Visit the *Dalton Transactions* website for more cutting-edge inorganic and organometallic research
www.rsc.org/dalton

Tuning the electronic structure of diboradiferrocenes†‡

Krishnan Venkatasubbaiah, Thilagar Pakkirisamy, Roger A. Lalancette and Frieder Jäkle*

Received 5th December 2007, Accepted 14th January 2008

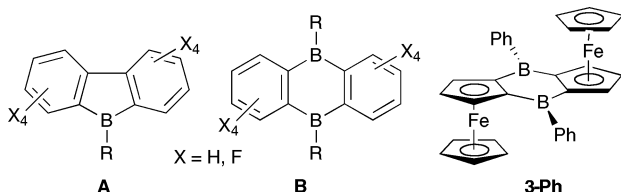
First published as an Advance Article on the web 10th July 2008

DOI: 10.1039/b718789k

A series of diboradiferrocenes with different aryl substituents was prepared through reaction of *B,B*-dichlorodiboradiferrocene **2** with arylcopper and Grignard reagents. The mesityl and pentafluorophenyl derivatives, **3-Mes** and **3-Pf**, were fully characterized by multinuclear NMR, MALDI-TOF mass spectrometry and X-ray crystallography, and their electronic structure was examined by UV-visible spectroscopy and cyclic voltammetry. A comparison of the data for **3-Mes** and **3-Pf** with those of the parent compound **3-Ph** revealed the importance of electronic and steric effects of the substituents on the electronic structure of the compounds and ultimately the degree of electronic interaction between the two ferrocene moieties. An unusually large redox splitting of $\Delta E = 703$ mV was determined from the cyclic voltammogram of **3-Pf**.

Introduction

The incorporation of boron into conjugated cyclic π -systems continues to be an attractive research objective, both from a synthetic perspective and due to the unusual optical and electronic properties that are commonly encountered.¹ The possibility of enhancing the Lewis acidity of organoboranes and thereby the efficiency in catalysis and chemosensor applications is an intriguing aspect that has attracted much interest. The working hypothesis is that, for example, in borole or diborabenzene derivatives participation of the empty p_π orbital on boron in what would become an antiaromatic $4n$ π -electron system is energetically unfavorable; the ensuing diminished p_π - π overlap in turn leads to enhanced Lewis acidity of the boron centers.²⁻⁴ Among the most easily accessible and thus most extensively studied examples are fused boracycles such as borafluorene (**A**)^{3,5} and diboraanthracene (**B**)^{2,4,6} derivatives. While these and related species have in the past been used primarily as building blocks for the generation of (multi-decker) sandwich complexes,⁷ much recent attention has focused on the superior performance of fluorinated derivatives as highly potent activators in Ziegler-Natta type olefin polymerization processes.^{3,4,8}



We have recently reported a new type of boracycle, the diboradiferrocene **3-Ph** in which, similar as in diboraanthracenes, two tri-coordinate boryl groups are incorporated into a six-

membered ring system.⁹⁻¹¹ However, instead of *ortho*-phenylene groups, two redox-active *ortho*-ferrocenylene moieties are fused to this central ring system. The preparation of **3-Ph** involves treatment of 1,1'-bis(trimethylstannyl)ferrocene with PhBCl_2 . A rearranged 1-stannyl-2-borylferrocene^{12,13} is initially formed, which in the presence of Al as a catalyst slowly reacts further to give the final product. The essentially air-stable bifunctional Lewis acid **3-Ph** displays interesting redox behavior as a result of effective electronic communication between the two iron centers *via* the tri-coordinate boron bridge.^{9,11} Moreover, oxidation of the ferrocene moieties leads to enhanced Lewis acidity of the organoborane sites.¹⁰ Given these highly unusual properties of **3-Ph** we set out to develop an alternative, more general methodology for the synthesis of diboradiferrocenes. We report here a novel modular synthetic approach, in which we take advantage of the facile reaction of the new halogen-substituted diboradiferrocene $\text{fc}_2\text{B}_2\text{Cl}_2$ (**2**) for the preparation of a family of diboradiferrocenes with tunable properties.

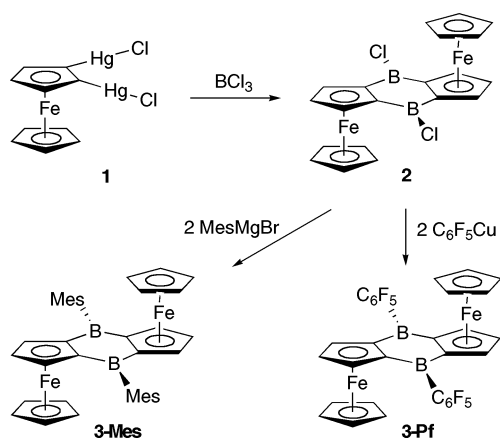
Results and discussion

Initial studies on the reactivity of boron halides toward 1,2-bis(trimethylstannyl)ferrocene¹⁴ revealed large quantities of products, in which the boryl groups are attached at the 1,1'-positions of ferrocene based on ¹H NMR screening. As noted above, rearrangements of this type allowed us to prepare 1-stannyl-2-borylferrocenes from 1,1'-bis(trimethylstannyl)-ferrocene with exceptionally high selectivity.¹² However, such a reactivity pattern is undesirable in the current case since it prevents clean conversion of 1,2-bis(trimethylstannyl)-ferrocene to the desired 1,2-disubstituted products. To circumvent these issues we decided to investigate as an alternative precursor the 1,2-bis(chloromercurio)ferrocene derivative (**1**), which is accessible with perfect retention of the 1,2-substitution pattern by reaction of 1,2-bis(trimethylstannyl)ferrocene with HgCl_2 .¹⁴ Compound **1** was treated with BCl_3 in 1,2-dichloroethane and the mixture kept at 110 °C for 12 h (Scheme 1). A dark red powder was isolated upon removal of the solvents. Recrystallization from hot hexanes

Department of Chemistry, Rutgers University-Newark, 73 Warren Street, Newark, NJ, 07102, USA. E-mail: fjaekle@rutgers.edu; Fax: +1 973 353 1264; Tel: +1 973 353 5064

† Based on the presentation given at Dalton Discussion No. 11, 23–25 June 2008, University of California, Berkeley, USA.

‡ CCDC reference numbers 669587–669589. For crystallographic data in CIF or other electronic format see DOI: 10.1039/b718789k



Scheme 1 Synthesis of diboradiferrocene derivatives 3.

afforded the spectroscopically pure dichlorodiboradiferrocene (**2**) as a dark red crystalline solid in a yield of *ca.* 38%.

Single crystals of **2** were obtained from a solution in hexanes at room temperature. Two different molecules of **2** were found in the unit cell. One of them sits on an inversion center (**2-A**, not shown), but the two halves of the other molecule are not symmetry related (**2-B**, Fig. 1). The most striking feature is the apparent puckering of the bridging dibora-*s*-indacene ligand, which was also observed for the phenyl derivative, **3-Ph**.⁹ This unusual geometric feature is not found for the respective diboraanthracene derivatives, but is a result of the bending of the individual electron-deficient boryl groups toward iron. The latter effect has been attributed by Wagner and Holthausen to a delocalized through-space interaction that involves the iron, boron, and the Cp rings based on DFT calculations on the monoborylated species FcBH_2 .¹⁵ The tilting of the dibora bridge with respect to the substituted Cp rings is considerably smaller for **2** (**2-A**, 9.2°; **2-B**, 13.2/13.7°) than for **3-Ph** (15.9°).

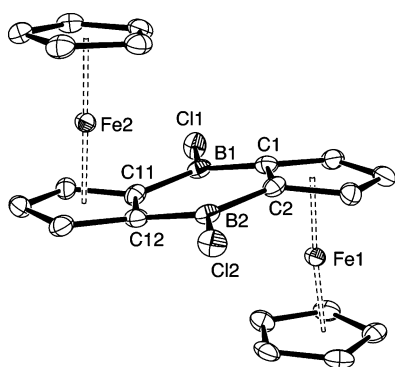


Fig. 1 Molecular structure of **2-B**; only one of two independent molecules in the unit cell is shown and hydrogen atoms are omitted for clarity. Selected interatomic distances (Å) and angles (°): B(1)–C(1) 1.526(5), B(1)–C(11) 1.543(5), B(2)–C(2) 1.533(5), B(2)–C(12) 1.528(5), B(1)–Cl(1) 1.783(3), B(2)–Cl(2) 1.784(3), C(1)–B(1)–C(11) 119.0(3), C(2)–B(2)–C(12) 119.4(3), Fe(1)⋯B(1) 2.984, Fe(1)⋯B(2) 3.021, Fe(2)⋯B(1) 3.025, Fe(2)⋯B(2) 2.994, B(1)⋯B(2) 3.015, Fe(1)⋯Fe(2) 5.201, Cp//Cp 2.9 and 1.0, Cp_{center}⋯Cp_{center} 3.300 and 3.312, Cp_{cent}–C(1)–B(1) 167.0, Cp_{cent}–C(2)–B(2) 167.6, Cp_{cent}–C(11)–B(1) 167.7, Cp_{cent}–C(12)–B(2) 166.7, (C1–C5)//C(1)C(2)B(1)B(2)C(11)C(12) 13.7, (C11–C15)//C(1)C(2)B(1)B(2)C(11)C(12) 13.2.

Compound **2** serves as a versatile precursor to other diboradiferrocene derivatives through nucleophilic replacement of the chlorine substituents as shown in Scheme 1. Reaction with MesMgBr (Mes = 2,4,6-trimethylphenyl) at 110 °C in toluene gave **3-Mes** as a dark red air-stable solid, which was purified by column chromatography on silica gel. Similarly, highly selective replacement of the chlorine substituents with C_6F_5 groups was accomplished by treatment of **2** with pentafluorophenyl copper in toluene at 50 °C. Recrystallization from toluene/hexanes mixtures gave pure **3-Mes** and **3-Pf** as dark red crystalline solids in yields of *ca.* 56 and 68%, respectively. The new diboradiferrocenes were fully characterized by multinuclear NMR, MALDI-TOF mass spectrometry and X-ray crystallography, and their electronic structure was examined by UV-visible spectroscopy and cyclic voltammetry.

The ^{11}B NMR spectra of **3-Mes** and **3-Pf** display broad signals at δ 62.2 and 52.7, respectively, in the typical region of triarylboranes (cf. **3-Ph** δ 57.7). The ferrocene region of the ^1H NMR spectra is indicative of the *ortho*-substitution pattern as evident from the presence of a doublet and a triplet in a 2:1 intensity ratio. In CDCl_3 as the solvent, the triplet is slightly downfield (**3-Mes** δ 4.98, **3-Pf** δ 5.12; cf. **3-Ph** δ 5.05) from the doublet (**3-Mes** δ 4.71, **3-Pf** δ 4.77; cf. **3-Ph** δ 4.89); all protons and carbon atoms for the substituted Cp rings are strongly deshielded relative to ferrocene as expected due to the π -acceptor effect of the tricoordinate boron. The MALDI-TOF spectra of **3-Mes** and **3-Pf** show clear evidence of the molecular ion peaks, thereby confirming the dimeric structures.

The availability of a series of diboradiferrocenes that feature aryl substituents of different steric and electronic nature provides a unique opportunity to examine substituent effects on the geometric parameters by single crystal X-ray diffraction. Plots of the X-ray crystal structures of **3-Mes** and **3-Pf** are shown in Fig. 2 and selected geometric parameters are compared in Table 1 with those of the parent phenyl-substituted molecule **3-Ph**. Compound **3-Mes** shows two independent molecules in the unit cell, both of which sit on crystallographic inversion centers as does the single unique molecule of **3-Pf**. While the bond lengths and angles are generally similar for **3-Mes** and **3-Pf**

Table 1 Comparison of selected interatomic distances (Å) and angles (°) for **3-Mes** and **3-Pf** with those of **3-Ph**

Compound	3-Mes		3-Pf	3-Ph^a
	Molecule A	Molecule B		
B–C _{Cp}	1.541(7)	1.554(7)	1.537(3)	1.546(2)
B–C _{Cp}	1.547(7)	1.531(7)	1.540(3)	1.546(2)
B–C _{Ph}	1.571(7)	1.579(7)	1.585(3)	1.564(2)
C _{Cp} –B–C _{Cp}	114.9(4)	115.4(4)	116.9(2)	115.8(1)
Fe⋯B	3.124	3.156	3.030	3.032
Fe⋯B*	3.127	3.112	3.053	2.957
B⋯B*	3.126	3.110	3.072	3.103
Fe⋯Fe*	5.413	5.442	5.251	5.123
Cp//Cp tilt	4.1	5.5	3.4	1.2
Cp _{cent} ⋯Cp _{cent}	3.317	3.310	3.311	3.308
Cp _{cent} –C _i –B	172.6	172.6	169.1	167.9
Cp _{cent} –C _i –B*	172.2	172.1	167.9	164.4
Cp//C ₄ B ₂	7.9	7.8	12.6	15.9
Ph//C ₄ B ₂	58.3	60.7	47.9	53.4

^a Data from ref. 9.

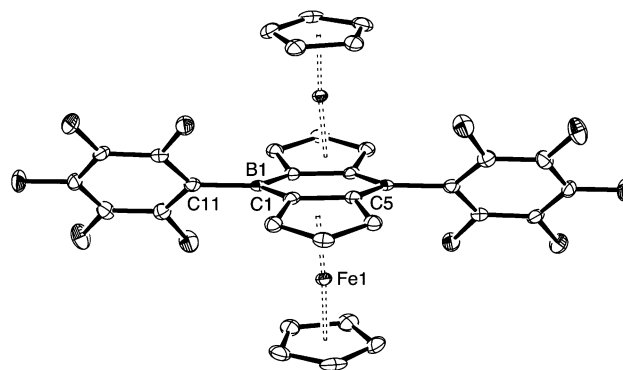
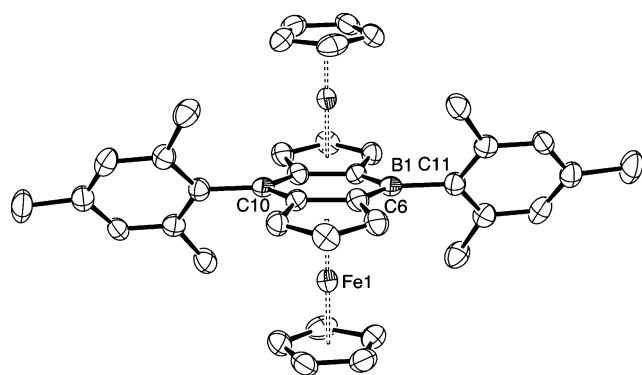


Fig. 2 ORTEP plots of **3-Mes** (left) and **3-Pf** (right) with thermal ellipsoids at the 50% probability level. Only one of two independent molecules in the unit cell is shown for **3-Mes**, and a disordered CDCl_3 solvent molecule is omitted. Hydrogen atoms are omitted for clarity.

and comparable to those of **3-Ph**, there are clear differences in the interplanar angles between the central diborabenzene and the Cp rings. The tilt angle is considerably smaller for **3-Mes** with 7.8 and 7.9° for the two independent molecules in comparison to the highly tilted parent compound **3-Ph** (15.9°), while the angle found for **3-Pf** lies in-between at 12.6°. Similarly, the individual boryl groups are more strongly bent out of the Cp plane for **3-Ph** (12.1 and 15.6°) than for **3-Mes** (7.9 to 7.4°) and **3-Pf** (10.9, 12.1°). Based only on electronic considerations a different order would have been expected. Given that the C_6F_5 moieties are the least and the mesityl groups the most strongly electron donating substituents, the most electron deficient boron centers in **3-Pf** should interact most strongly with Fe, and hence the largest angles should be observed for **3-Pf**, followed by **3-Ph** and **3-Mes**. However, experimentally the largest bending is observed for **3-Ph** and this apparent discrepancy indicates that steric factors also play an important role and ultimately prevent more pronounced $\text{Fe} \cdots \text{B}$ interactions in **3-Pf** and possibly also in **3-Mes**, for which the small angles can be rationalized on both steric and electronic grounds. Steric effects are also evident from a comparison of the Cp//Cp tilt angles of the individual ferrocene units. Due to the steric bulk of the mesityl groups large Cp//Cp tilt angles are found for **3-Mes** with 4.1 and 5.5°. Importantly, even for **3-Pf** the Cp//Cp tilting of 3.4° is significantly more pronounced than for **3-Ph** (1.2°).

One of the most interesting aspects of compound **3-Ph** is the strong electronic communication between the ferrocene moieties that is evident from two separate redox events relating to oxidation of the first and second ferrocene moiety with an unusually large redox splitting of 510 mV.^{9,11} The cyclic voltammograms of **3-Mes** and **3-Pf** are displayed in Fig. 3 together with that of **3-Ph** and the data are summarized in Table 2. For both **3-Mes** and **3-Pf** two redox waves are observed similar to those of **3-Ph**. The second oxidation wave shows far better electrochemical reversibility for

Table 2 Comparison of CV data for **3-Mes** and **3-Pf** with **3-Ph**^a

	$E_{1/2}$ (1)	ΔE_{p1}	$E_{1/2}$ (2)	ΔE_{p2}	ΔE (2–1)
3-Ph ^b	60	79	570	120	510
3-Mes	73	90	652	102	579
3-Pf	244	90	947	137	703

^a Data are reported in mV relative to the ferrocene/ferrocenium couple.

^b Data from ref. 9.

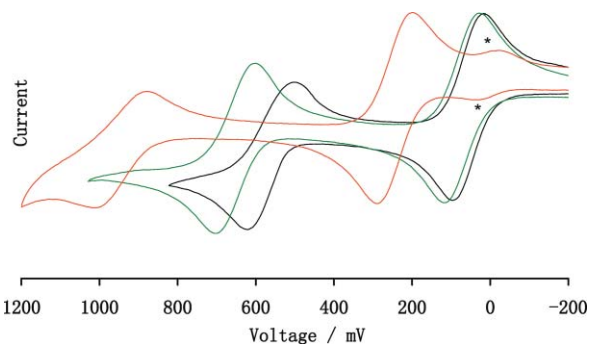


Fig. 3 Overlay of the cyclic voltammograms of **3-Ph** (black), **3-Mes** (green), and **3-Pf** (red). The data are reported vs. FcH/FcH^+ . Conditions: ca. 1×10^{-3} M solutions in 0.05M $[\text{Bu}_4\text{N}][\text{B}(\text{C}_6\text{F}_5)_4]/\text{CH}_2\text{Cl}_2$ as the supporting electrolyte, 100 mV s^{-1} . * denotes a trace of ferrocene.

3-Mes than for **3-Pf** and **3-Ph**. This effect is attributed to the comparatively higher solubility of **3-Mes**, assuming a similar trend for the mono- and dicationic species in the electrolyte solution as for the neutral species. While the first redox wave for **3-Mes** ($E_{1/2} = 73$ mV vs. Fc/Fc^+) is found at a potential similar to that of **3-Ph** and hence at only a slightly higher potential than ferrocene itself, for **3-Pf** this first oxidation occurs at a considerably higher potential of $E_{1/2} = 244$ mV. The latter is consistent with attachment of the electron withdrawing C_6F_5 moieties and in reasonably good agreement with data reported by Piers *et al.* for $\text{FcB}(\text{C}_6\text{F}_5)_2$ (450 mV in trifluorotoluene/ $\text{Bu}_4\text{N}[\text{B}(\text{C}_6\text{F}_5)_4]$).¹⁶

Remarkably, the second oxidation event occurs for both **3-Mes** and **3-Pf** at higher potential than for **3-Ph**. Consequently, the redox splitting for **3-Mes** ($\Delta E = 579$ mV) and especially that of **3-Pf** ($\Delta E = 703$ mV) is larger than that determined for **3-Ph**. A similarly large redox coupling has recently been reported for the ferrocenylborane polymer $\{1,1'\text{-fc-B}(\text{Mes})-\}_n$ with $\Delta E = 705$ mV in $\text{Bu}_4\text{N}[\text{B}(\text{C}_6\text{F}_5)_4]/\text{CH}_2\text{Cl}_2$ as the electrolyte.¹⁷ In the case of this polymer, however, a very high second oxidation potential is to be expected: after oxidation of alternating ferrocene moieties along the polymer chain during the first oxidation wave, the remaining ferrocene groups face two (rather than one) neighboring oxidized ferrocenyl moieties, both of which are expected to act as electron withdrawing groups that in turn enhance the electron deficient nature of the boron centers.¹⁸ In agreement with this analysis is that a more moderate redox coupling of $\Delta E = 422$ mV was found for the respective diferrocenylborane Fc_2BMe s. The large redox coupling

for **3-Pf** is thus indicative of generation of highly electron-deficient boron centers due to the presence of both electron withdrawing C_6F_5 and ferrocenyl moieties after mono-oxidation.

The analysis given above does not explain the enhanced redox splitting for **3-Mes** relative to **3-Ph**. Our interpretation of this seeming inconsistency takes into consideration the steric crowding in **3-Mes** as evident from the X-ray crystal structure analysis. A comparison of the interplanar angles between the C_4B_2 ring and the (substituted) phenyl rings shows that the largest angles are found for **3-Mes** (58.3° and 60.7°), followed by **3-Ph** (53.4°) and **3-Pf** (47.9°), suggesting that π -overlap between the boron p orbital and the exocyclic substituents is least favorable for **3-Mes**.¹⁹ Similar observations have been made for Fc_2BMe_6 , for which the mesityl group makes an angle of 61.2° with the trigonal boron moiety.¹⁷ Importantly, upon mono-oxidation of **3-Ph** to $[3-Ph]^+$ this interplanar angle is considerably lowered (e.g. for $[3-Ph]^+PF_6^-$ angles of $36.3/45.8^\circ$ and $36.2/45.5^\circ$ are found for two independent unsymmetric molecules; for $[3-Ph]^+SbF_6^-$: $38.8/44.6^\circ$).^{10,11} This change in geometry presumably is a result of enhanced π -bonding between boron and the phenyl groups that compensates for the decreased π -interaction with the oxidized ferrocene moieties. However, such a planarization ought to be unfavorable in the case of the mesityl-substituted derivative, which may explain why the second oxidation of **3-Mes** occurs at higher potential than that of the sterically less congested derivative **3-Ph**.

Finally, we examined the UV-visible spectra of compounds **3-Mes** and **3-Pf**, and a comparison with the parent molecule **3-Ph** is shown in Fig. 4. The longest wavelength absorption, which is attributed to a dd transition of the ferrocene moieties with significant charge transfer character,¹² is most bathochromic for the pentafluorophenyl-substituted compound **3-Pf** ($\lambda_{max} = 527$ nm). However, surprisingly, the absorption maximum of the mesityl derivative **3-Mes** ($\lambda_{max} = 519$ nm) is also considerably red-shifted relative to that of **3-Ph** ($\lambda_{max} = 498$ nm) and approaches that of **3-Pf**.²⁰ This order reflects that of the CV data, and thus further suggests that electronic interaction through the diborabenzene linker is promoted by either electron withdrawing substituents such as C_6F_5 groups or by bulky aryl groups that adopt a conformation orthogonal to the diborabenzene and hence do not participate significantly in π -bonding with the empty p -orbitals on boron. The increased Cp//Cp ring tilting for **3-Mes** may also impact the absorption properties, and a correlation of the tilt angle in strained [1]ferrocenophanes with λ_{max} has been suggested by Manners *et al.*²¹

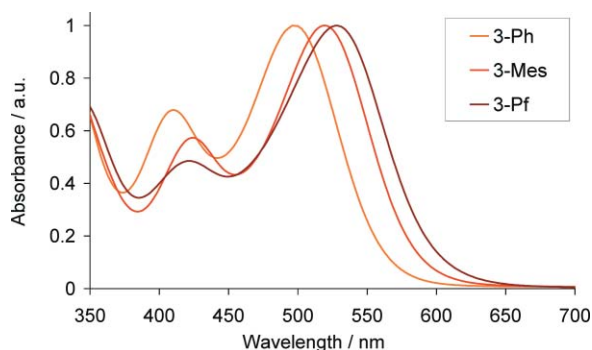


Fig. 4 Overlay of the UV-visible spectra of **3-Mes**, **3-Pf**, and **3-Ph**.

Conclusions

We have developed a new synthetic approach to diboradiferrocene species starting from the chloro-substituted boracycle **2**, which serves as a versatile precursor to other derivatives through nucleophilic substitution reactions. As shown here, the chlorine substituents can be replaced with different aryl groups to tune the Lewis acidity of the bridging boryl groups and consequently influence the degree of electronic interaction between the two ferrocene moieties as evidenced by an enhanced redox coupling and red-shifted absorption maximum for **3-Pf** relative to **3-Ph**.²² Importantly, we expect that the binding behavior towards anions and the ability to act as Lewis acid catalysts for organic transformations can be addressed in a similar manner; these are new opportunities that we are currently further pursuing.

Experimental

1,2-Bis(chloromercury)ferrocene¹⁴ and pentafluorophenyl copper²³ were prepared according to literature procedures, and mesitylmagnesium bromide (0.5 M in THF) was synthesized from bromomesitylene and Mg in THF. BCl_3 (1M in hexanes) was purchased from Acros. All reactions and manipulations involving reactive organoboron species were carried out under an atmosphere of prepurified nitrogen using either Schlenk techniques or an inert-atmosphere glovebox (Innovative Technologies). Hydrocarbon and chlorinated solvents were purified using a solvent purification system (Innovative Technologies), and the chlorinated solvents were subsequently degassed *via* several freeze-pump-thaw cycles.

499.9 MHz 1H NMR, 125.7 MHz ^{13}C NMR, 470.4 MHz ^{19}F NMR and 160.4 MHz ^{11}B NMR spectra were recorded on a Varian INOVA NMR spectrometer (Varian Inc., Palo Alto, CA) equipped with a 5 mm dual broadband gradient probe (Nalorac, Varian Inc., Martinez, CA). Solution 1H and ^{13}C NMR spectra were referenced internally to the solvent signals. ^{19}F NMR spectra were referenced externally to $\alpha, \alpha', \alpha''$ -trifluorotoluene (0.05% in C_6D_6 ; $\delta = -63.73$) and ^{11}B NMR spectra to $BF_3 \cdot OEt_2$ ($\delta = 0$) in C_6D_6 .

Cyclic voltammetry measurements were carried out with a BAS CV-50W analyzer. The three-electrode system consisted of a Au disk as working electrode, a Pt wire as secondary electrode, and a Ag wire as the pseudo-reference electrode. The voltammograms were recorded in dichloromethane containing 0.05 M $[Bu_4N][B(C_6F_5)_4]$ as the supporting electrolyte. Data were acquired with decamethylferrocene as an internal reference and are reported relative to the ferrocene/ferrocenium couple (+610 mV with 0.1 M $[Bu_4N][B(C_6F_5)_4]$ in CH_2Cl_2 vs. the decamethylferrocene/decamethylferrocenium couple).

UV-visible absorption data were acquired on a Varian Cary 500 UV-vis/NIR spectrophotometer. Solutions were prepared using a microbalance (± 0.1 mg) and volumetric glassware and then charged into quartz cuvettes with sealing screw caps (Starna) inside the glovebox.

GC-MS spectra were acquired on a Hewlett Packard HP 6890 Series GC system equipped with a series 5973 mass selective detector and a series 7683 injector. A temperature profile with a heating rate of $20^\circ C \text{ min}^{-1}$ from $50^\circ C$ to $300^\circ C$ was used. Mass spectral data in FAB positive ion mode with NBA (4-nitrobenzylalcohol) as matrix were obtained at the Michigan State

University Mass Spectrometry Facility, which is supported, in part, by a grant (DRR-00480) from the Biotechnology Research Technology Program, National Center for Research Resources, National Institutes of Health. MALDI-TOF measurements were performed on an Applied Biosystems 4700 Proteomics Analyzer in reflectron (+) mode with delayed extraction. Benzo[a]pyrene was used as the matrix (10 mg mL⁻¹ in toluene). Samples were prepared in toluene (10 mg mL⁻¹), mixed with the matrix in a 1 : 10 ratio, and then spotted on the wells of a sample plate inside a glove box. Elemental analyses were obtained from Quantitative Technologies Inc., Whitehouse, NJ.

Details of X-ray diffraction experiments and crystal structure refinements for **3-Mes** and **3-Pf** are provided in Table 3. Data were collected at 100(2) K on a Bruker SMART APEX CCD diffractometer using Cu K α (1.54178 Å) radiation. Numerical absorption corrections were applied in all cases. The structures were solved using direct methods, completed by subsequent difference Fourier syntheses and refined by full matrix least squares procedures on F^2 . All non-hydrogen atoms were refined with anisotropic displacement coefficients. The H atoms were placed at calculated positions and were refined as riding atoms. All software and source scattering factors are contained in the SHELXTL program package.²⁴ There is a disordered solvent chloroform molecule included in the crystal of **3-Mes**. It was split over two positions and refined anisotropically. The occupancy factors for the major domain of the CHCl₃ site refined to 0.643. Crystallographic data for the structures of **2**, **3-Mes** and **3-Pf** have been deposited with the Cambridge Crystallographic Data Center as supplementary publication no. CCDC 669587–669589.

Copies of the data can be obtained free of charge on application to CCDC, 12 Union Road, Cambridge CB21EZ, UK (fax: (+44) 1223-336-033; email: deposit@ccdc.cam.ac.uk).

Synthesis of Fc₂B₂Cl₂ (**2**)

To a suspension of 1,2-bis(chloromercury)ferrocene (**1**) (8.00 g, 12.2 mmol) in dichloroethane (180 mL) in a Teflon-stoppered glass tube was added BCl₃ (14 mL, 1M solution in hexanes) inside a glove box. The tube was closed and immersed into an oil bath at 110 °C for 12 h. After cooling to room temperature the volatile components were removed under reduced pressure. The product was extracted with toluene, hexanes were added, and the mixture was filtered. The solvents were removed under high vacuum to give a red solid. Recrystallization from hot hexanes gave **2** as a dark red crystalline solid. Yield: 1.08 g (38%). X-Ray quality crystals were obtained from a hexanes solution at room temperature. For **2**: ¹H NMR (499.9 MHz, CDCl₃, 25 °C) δ 5.12 (t, J = 2.5 Hz, 2H, Cp-4), 5.05 (d, J = 2.5 Hz, 4H, Cp-3,5), 4.11 (s, 10H, free Cp). ¹H NMR (499.9 MHz, C₆D₆, 25 °C) δ 5.04 (d, J = 2.5 Hz, 4H, Cp-3,5), 4.69 (t, J = 2.5 Hz, 2H, Cp-4), 3.88 (s, 10H, free Cp). ¹³C NMR (125.7 MHz, C₆D₆, 25 °C) δ 80.3 (Cp-3,5), 80.1 (Cp-4), 71.4 (free Cp), n.o. *ipso*-Cp-B. ¹¹B NMR (160.4 MHz, C₆D₆, 25 °C) δ 49.9 ($w_{1/2}$ = 600 Hz). UV-Vis (CH₂Cl₂, 2.5 × 10⁻⁴ M) λ_{max} (ϵ) = 492 nm (4540 M⁻¹ cm⁻¹), 405 (3730 M⁻¹ cm⁻¹).

Synthesis of Fc₂B₂Mes₂ (**3-Mes**)

A solution of mesitylmagnesium bromide (0.8 mL, 0.5 M in THF) was transferred to a Teflon-stoppered glass tube and the solvent

Table 3 Details of X-ray crystal structure determinations

Compound	2	3-Mes	3-Pf
Formula	C ₂₀ H ₁₆ B ₂ Cl ₂ Fe ₂	C ₃₉ H ₃₉ B ₂ Cl ₃ Fe ₂	C ₃₂ H ₁₆ B ₂ F ₁₀ Fe ₂
<i>M</i>	460.55	747.37	723.77
Crystal system	Triclinic	Triclinic	Monoclinic
Space group	<i>P</i> -1	<i>P</i> -1	<i>C</i> 2/ <i>c</i>
<i>a</i> /Å	8.1595(2)	11.2730(2)	23.7946(2)
<i>b</i> /Å	12.9933(2)	11.9306(2)	7.0879(1)
<i>c</i> /Å	14.0037(2)	14.7300(2)	18.0370(2)
α /°	112.665(2)	90.4950(10)	90
β /°	97.722(2)	103.3200(10)	119.329(2)
γ /°	95.855(2)	114.8210(10)	90
<i>V</i> /Å ³	1338.24(7)	1737.22(5)	2652.09(5)
<i>Z</i>	3	2	4
ρ_{calc} /g cm ⁻³	1.714	1.429	1.813
μ (Cu K α)/mm ⁻¹	15.776	9.018	9.645
Crystal size/mm	0.49 × 0.34 × 0.29	0.23 × 0.21 × 0.06	0.26 × 0.19 × 0.11
θ range/°	3.74 to 68.39	3.11 to 59.99	4.26 to 67.89
Limiting indices	-9 ≤ <i>h</i> ≤ 9 -15 ≤ <i>k</i> ≤ 15 -16 ≤ <i>l</i> ≤ 16	-12 ≤ <i>h</i> ≤ 12 -12 ≤ <i>k</i> ≤ 13 -16 ≤ <i>l</i> ≤ 13	-28 ≤ <i>h</i> ≤ 28 -8 ≤ <i>k</i> ≤ 8 -21 ≤ <i>l</i> ≤ 21
Refins collected	8355	10934	13982
Unique refins	4409	4720	2400
<i>R</i> (int)	0.0358	0.0399	0.0431
Data/restraints/parameters	4409/0/352	4720/0/450	2400/0/208
GOF on F^2	1.051	1.062	1.042
Final <i>R</i> indices	<i>R</i> 1 = 0.0462	<i>R</i> 1 = 0.0528	<i>R</i> 1 = 0.0301
[<i>I</i> > 2 σ (<i>I</i>)] ^a	<i>wR</i> 2 = 0.1198	<i>wR</i> 2 = 0.1468	<i>wR</i> 2 = 0.0756
<i>R</i> indices (all data) ^a	<i>R</i> 1 = 0.0474	<i>R</i> 1 = 0.0660	<i>R</i> 1 = 0.0337
	<i>wR</i> 2 = 0.1211	<i>wR</i> 2 = 0.1595	<i>wR</i> 2 = 0.0778
Peak/hole/e Å ⁻³	1.465/-0.607	0.696/-0.740	0.493/-0.268

^a $R1 = \sum \|F_o - |F_c|\| / \sum |F_o|$; $wR2 = \{\sum [w(F_o^2 - F_c^2)^2] / \sum [w(F_o^2)^2]\}^{1/2}$.

was removed under high vacuum. The residue was suspended in toluene (5 mL), and a solution of **2** (40.5 mg, 0.088 mmol) in toluene was added. The reaction mixture was kept stirring at 110 °C for 12 h. After cooling to room temperature the solvent was removed under high vacuum. The compound was extracted with a toluene/hexanes mixture and passed through a silica gel column (hexanes:CH₂Cl₂ 9:1 as eluent). The product was recrystallized from a toluene/hexanes mixture at -35 °C. Yield: 31 mg (56%). X-Ray quality crystals were obtained by slow evaporation of a CDCl₃ solution. For **3-Mes**: ¹H NMR (499.9 MHz, CDCl₃, 25 °C) δ 6.98 (s, 4H, *meta*-Mes), 4.98 (t, *J* = 2.5 Hz, 2H, Cp-4), 4.71 (d, *J* = 2.5 Hz, 4H, Cp-3,5), 4.03 (s, 10H, free Cp), 2.56 (s, 12H, *ortho*-Me), 2.39 (s, 6H, *para*-Me). ¹³C NMR (125.7 MHz, CDCl₃, 25 °C) δ 140.5 (*ortho*-Mes), 139.4 (br, *ipso*-B-Mes), 137.3 (*para*-Mes), 128.0 (*meta*-Mes), 83.3 (br, *ipso*-Cp-B), 81.3 (Cp-3,5), 79.2 (Cp-4), 70.4 (free Cp), 24.3 (*ortho*-Me), 21.4 (*para*-Me). ¹¹B NMR (160.4 MHz, CDCl₃, 25 °C) δ 62.2 (*w*_{1/2} = 1600 Hz). UV-Vis (CH₂Cl₂, 2.4 × 10⁻⁴ M) λ_{max} (ε) = 519 nm (5560 M⁻¹ cm⁻¹), 424 (3190 M⁻¹ cm⁻¹). FAB-MS (NBA): *m/z* (%) 628 (100) [M⁺], 563 (5) [M⁺-Cp], 509 (7) [M⁺-Mes]; small amounts of higher aggregates and their fragments are found: 1256 (5) [M₂⁺]. MALDI-TOF MS: *m/z* 628.1934 (calcd for ¹²C₃₈¹H₃₈¹¹B₂⁵⁶Fe₂: 628.1858). Calcd for C₃₈H₃₈B₂Fe₂·C₇H₈ (1 equiv toluene by ¹H NMR): C 75.05, H 6.44%; found C 74.62, H 6.51%.

Synthesis of Fc₂B₂(C₆F₅)₂ (**3-Pf**)

To a solution of **2** (30 mg, 0.065 mmol) in toluene (2 mL) in a Teflon-stoppered glass tube was added pentafluorophenyl copper (30 mg, 0.13 mmol) in toluene (2 mL) inside a glove box. The reaction mixture was heated to 50 °C for 12 h. After cooling to room temperature the reaction mixture was filtered and the solvents were removed under reduced pressure. The residue shows about 95% purity by ¹H and ¹⁹F NMR and was recrystallized from toluene/hexanes mixture at -35 °C. Yield: 32 mg (68%). X-Ray quality crystals were obtained from a toluene/hexanes (3:1) mixture at room temperature. For **3-Pf**: ¹H NMR (499.9 MHz, CDCl₃, 25 °C) δ 5.12 (t, *J* = 2.5 Hz, 2H, Cp-4), 4.77 (br, 4H, Cp-3,5), 4.14 (s, 10H, free Cp). ¹⁹F NMR (470.4 MHz, CDCl₃, 25 °C) δ -129.3 (dd, *J* = 11, 25 Hz, *ortho*-F), -153.9 (t, *J* = 20, *para*-F), -162.9 (br m, *meta*-F). ¹³C NMR (125.7 MHz, CDCl₃, 25 °C) δ 147.1 (d, *J*(C,F) = 252 Hz, *ortho*-C₆F₅), 141.8 (d, *J*(C,F) = 250 Hz, *para*-C₆F₅), 137.8 (d, *J*(C,F) = 247 Hz, *meta*-C₆F₅), 113.8 (br, *ipso*-C₆F₅), 82 (very br, *ipso*-Cp-B), 81.8 (d, *J*(C,F) = 3.9 Hz, Cp-3,5), 80.9 (Cp-4), 70.7 (free Cp). ¹¹B NMR (160.4 MHz, CDCl₃, 25 °C) δ 52.7 (*w*_{1/2} = 1280 Hz). UV-Vis (CH₂Cl₂, 2.5 × 10⁻⁴ M) λ_{max} (ε) = 527 nm (5460 M⁻¹ cm⁻¹), 420 (2650 M⁻¹ cm⁻¹). GC-MS (*m/z*, (%)): 724 [M⁺] (100). MALDI-TOF MS: *m/z* 723.9857 (calcd for ¹²C₃₂¹H₁₆¹¹B₂¹⁹F₁₀⁵⁶Fe₂: 723.9977). Calcd for C₃₂H₁₆B₂F₁₀Fe₂: C 53.10, H 2.23%; found C 53.01, H 2.08%.

Acknowledgements

We are grateful to the donors of the Petroleum Research Fund, administered by the American Chemical Society for support of this research and to the National Science Foundation for partial funding of an X-ray diffractometer (NSF CRIF-0443538). F.J. thanks the Alfred P. Sloan foundation for a research fellowship and the National Science foundation for a CAREER award (CHE-

0346828). We are grateful to Haiyan Li for acquisition of cyclic voltammetry data.

References

- W. Siebert, *Adv. Organomet. Chem.*, 1993, **35**, 187–210; C. E. Housecroft, *Compounds with Three- or Four-Coordinate Boron, Emphasizing Cyclic Systems*, in *Comprehensive Organometallic Chemistry*, ed. E. W. Abel, F. G. A. Stone, and G. Wilkinson, Pergamon Press, Oxford, 1995, pp. 129–195; G. E. Herberich, *Boron Rings Ligated to Metals in Comprehensive Organometallic Chemistry*, ed. E. W. Abel, F. G. A. Stone, and G. Wilkinson, Pergamon Press, Oxford, 1995, pp. 197–216; G. C. Fu, *Adv. Organomet. Chem.*, 2001, **47**, 101–119; F. Jäkle, *Boron: Organoboranes in Encyclopedia of Inorganic Chemistry*, ed. R. B. King, Wiley VCH, 2005, pp 560–598.
- J. J. Eisch and B. W. Kotowicz, *Eur. J. Inorg. Chem.*, 1998, 761–769; H. Braunschweig, I. Fernández, G. Frenkin and T. Kupfer, *Angew. Chem., Int. Ed.*, 2008, **47**, 1951–1954.
- P. A. Chase, W. E. Piers and B. O. Patrick, *J. Am. Chem. Soc.*, 2000, **122**, 12911–12912.
- M. V. Metz, D. J. Schwartz, C. L. Stern, P. N. Nickias and T. J. Marks, *Angew. Chem., Int. Ed.*, 2000, **39**, 1312–1316; M. V. Metz, D. J. Schwartz, C. L. Stern, T. J. Marks and P. N. Nickias, *Organometallics*, 2002, **21**, 4159–4168.
- R. Koester and G. Benedikt, *Angew. Chem.*, 1963, **75**, 419; C. K. Narula and H. Noeth, *J. Organomet. Chem.*, 1985, **281**, 131–134; S. Yamaguchi, T. Shirasaka, S. Akiyama and K. Tamao, *J. Am. Chem. Soc.*, 2002, **124**, 8816–8817; R. J. Wehmschulte, M. A. Khan, B. Twamley and B. Schiemenz, *Organometallics*, 2001, **20**, 844–849; P. E. Romero, W. E. Piers, S. A. Decker, D. Chau, T. K. Woo and M. Parvez, *Organometallics*, 2003, **22**, 1266–1274; R. J. Wehmschulte, A. A. Diaz and M. A. Khan, *Organometallics*, 2003, **22**, 83–92; P. A. Chase, L. D. Henderson, W. E. Piers, M. Parvez, W. Clegg and M. R. J. Elsegood, *Organometallics*, 2006, **25**, 349–357; A. Wakamiya, K. Mishima, K. Ekawa and S. Yamaguchi, *Chem. Commun.*, 2008, 579–581.
- R. Clement, *Fr. Compt. Rend.*, 1965, **261**, 4436–4438; W. Siebert, M. Schmidt and E. Gast, *J. Organomet. Chem.*, 1969, **20**, 29–33; P. Müller, S. Huck, H. Köppel, H. Pritzkow and W. Siebert, *Z. Naturforsch.*, 1995, **50**, 1476–1484; H. Akutsu, K. Kozawa and T. Uchida, *Acta Crystallogr., Sect. C*, 1996, **C52**, 991–993; H. Akutsu, K. Kozawa and T. Uchida, *Synth. Met.*, 1995, **70**, 1109–1110.
- P. Müller, B. Gangnus, H. Pritzkow, H. Schulz, M. Stephan and W. Siebert, *J. Organomet. Chem.*, 1995, **487**, 235–243; P. Müller, H. Pritzkow and W. Siebert, *J. Organomet. Chem.*, 1996, **524**, 41–47.
- V. C. Williams, C. Dai, Z. Li, S. Collins, W. E. Piers, W. Clegg, M. R. J. Elsegood and T. B. Marder, *Angew. Chem., Int. Ed.*, 1999, **38**, 3695–3698.
- K. Venkatasubbaiah, L. N. Zakharov, W. S. Kassel, A. L. Rheingold and F. Jäkle, *Angew. Chem., Int. Ed.*, 2005, **44**, 5428–5433.
- K. Venkatasubbaiah, I. Nowik, R. H. Herber and F. Jäkle, *Chem. Commun.*, 2007, 2154–2156.
- K. Venkatasubbaiah, A. Doshi, I. Nowik, R. H. Herber, A. L. Rheingold and F. Jäkle, *Chem.–Eur. J.*, 2008, **14**, 444–458.
- J. A. Gamboa, A. Sundararaman, L. Kakalis, A. J. Lough and F. Jäkle, *Organometallics*, 2002, **21**, 4169–4181.
- R. Boshra, A. Sundararaman, L. N. Zakharov, C. D. Incarvito, A. L. Rheingold and F. Jäkle, *Chem.–Eur. J.*, 2005, **11**, 2810–2824; R. Boshra, K. Venkatasubbaiah, A. Doshi, R. A. Lalancette, L. Kakalis and F. Jäkle, *Inorg. Chem.*, 2007, **46**, 10174–10186; R. Boshra, A. Doshi and F. Jäkle, *Angew. Chem., Int. Ed.*, 2008, **47**, 1134–1137.
- K. Venkatasubbaiah, J. W. Bats, A. L. Rheingold and F. Jäkle, *Organometallics*, 2005, **24**, 6043–6050.
- M. Scheibitz, M. Bolte, J. W. Bats, H.-W. Lerner, I. Nowik, R. H. Herber, A. Krapp, M. Lein, M. Holthausen and M. Wagner, *Chem.–Eur. J.*, 2005, **11**, 584–603.
- B. E. Carpenter, W. E. Piers, M. Parvez, G. P. A. Yap and S. J. Rettig, *Can. J. Chem.*, 2001, **79**, 857–867; B. E. Carpenter, W. E. Piers and R. McDonald, *Can. J. Chem.*, 2001, **79**, 291–295.
- M. Scheibitz, J. B. Heilmann, R. F. Winter, M. Bolte, J. W. Bats and M. Wagner, *Dalton Trans.*, 2005, 159–170; J. B. Heilmann, M. Scheibitz, Y. Qin, A. Sundararaman, F. Jäkle, T. Kretz, M. Bolte, H.-W. Lerner, M. C. Holthausen and M. Wagner, *Angew. Chem., Int. Ed.*, 2006, **45**, 920–925; J. B. Heilmann, Y. Qin, F. Jäkle, H. W. Lerner and M. Wagner, *Inorg. Chim. Acta*, 2006, **359**, 4802–4806.

- 18 For a discussion of the Lewis acidity enhancement of ferrocenylboranes upon oxidation of the iron centers see ref. 10.
- 19 The B–C_{ph} distances of 1.585(3) Å for **3-Pf** and of 1.571(7)/1.579(6) Å for **3-Mes** are longer than that of 1.564(2) Å for **3-Ph**, which is consistent with a decreased π -overlap of the empty p_x-orbital on boron with the mesityl and C₆F₅ substituents, respectively; however, the standard deviations for the B–C distances for **3-Mes** prevent any further conclusions.
- 20 In comparison, absorption maxima of 490 nm and 505 nm have been determined for Fc₂BMes and the polymer {1,1'-fc-B(Mes)-}_n, respectively; see ref. 17.
- 21 A. Berenbaum, H. Braunschweig, R. Dirk, U. Englert, J. C. Green, F. Jäkle, A. J. Lough and I. Manners, *J. Am. Chem. Soc.*, 2000, **122**, 5765–5774; D. E. Herbert, U. F. J. Mayer and I. Manners, *Angew. Chem., Int. Ed.*, 2007, **46**, 5060–5081.
- 22 For a more detailed discussion of the electronic communication *via* the diboron bridge in **3-Ph** see ref. 11.
- 23 A. Cairncross, H. Omura and W. A. Sheppard, *J. Am. Chem. Soc.*, 1971, **93**, 248–249; A. Cairncross, W. A. Sheppard, E. Wonchoba, W. J. Guildford, C. B. House and R. M. Coates, *Org. Synth.*, 1979, **59**, 122–131; A. Sundaraman, R. A. Lalancette, L. N. Zakharov, A. L. Rheingold and F. Jäkle, *Organometallics*, 2003, **22**, 3526–3532; A. Sundaraman and F. Jäkle, *J. Organomet. Chem.*, 2003, **681**, 134–142; F. Jäkle, *Dalton Trans.*, 2007, 2851–2858.
- 24 G. Sheldrick, *SHELXTL, Version 6.14*, Bruker AXS Inc., Madison, WI, 2004.